FREE-CONVECTIVE AND RADIATIVE HEAT TRANSFER ON A VERTICAL PLANE SURFACE

O. G. Martynenko, Yu. A. Sokovishin, and M. V. Shapiro

UDC 536.244

Calculations are carried out to determine the influence of radiation on the free-convective heat transfer of a vertical surface situated in a nonabsorbing medium. The known analytical and experimental data are compared, and a nomogram is proposed for the analysis of mixed convection.

Heat-transfer calculations for the high-temperature surfaces of equipment currently necessitate a simultaneous analysis of the influence of various kinds of heat transfer on the characteristics of the process. Of particular interest is the interaction of natural convection with radiation near a heated vertical surface. The complex heat-transfer processes involved here are accompanied by the absorption, emission, and scattering of radiation by the fluid [1, 2]. However, for not too high a surface temperature air can be regarded as devoid of the indicated properties and the influence of radiation included only in the heat balance at the wall. If the latter has a specified temperature, then the heat transfer for a nonabsorbing medium is determined independently for the radiative and convective components. For a given value of the wall heat flux such independence of the two heat-transfer modes does not hold. The heat flux from the wall is carried by the radiative component, which depends on the local temperature, as well as by the convective and conductive components. The latter determine the wall temperature and therefore affect the radiation.

Approximative methods have been used [3-7] to investigate the influence of radiation on the heat-transfer of a vertical plate in a free-convective boundary layer. Explicit heat-transfer relations are obtained by integral methods. They are rather bulky and do not mirror the effects of all the parameters on the heat-transfer process. In the present article we carry out a complete numerical solution of the problem over wide ranges of the defining criteria. The data of the numerical computations make it possible to determine the limits of applicability of the indicated results.

Let us consider laminar free-convective motion of a viscous incompressible fluid with constant physical properties in a boundary layer next to a vertical plane surface. To calculate the lift we use the Boussinesq approximation and neglect viscous dissipation. We assume that the wall is a diffuse gray radiator with emissivity ε, and for the radiative component we use the Stefan—Boltzmann law. Radiation takes place into a medium having a temperature T_∞ far from the surface.

The system of equations of motion and heat transfer in the boundary layer plus the boundary conditions has the form

$$u\frac{\partial u}{\partial x}+v\frac{\partial u}{\partial y}=\nu\frac{\partial^2 u}{\partial y^2}+g\beta(T-T_\infty), \tag{1}$$

$$u\frac{\partial T}{\partial x}+v\frac{\partial T}{\partial y}=a\frac{\partial^2 T}{\partial y^2}, \tag{2}$$

$$\frac{\partial u}{\partial x}+\frac{\partial v}{\partial y}=0, \tag{3}$$

$$\begin{gathered} u=v=0,\quad q_w=-\lambda\left(\frac{\partial T}{\partial y}\right)_w+\sigma\varepsilon(T_w^4-T_\infty^4)\quad \text{at}\quad y=0,\\ u=0,\quad T=T_\infty\quad \text{for}\quad y\to\infty. \end{gathered} \tag{4}$$

A. V. Lykov Institute of Heat and Mass Transfer, Academy of Sciences of the Belorussian SSR, Minsk.
Translated from Inzhenerno-Fizicheskii Zhurnal, Vol. 32, No. 6, pp. 1071-1079, June, 1977. Original article submitted May 18, 1976.

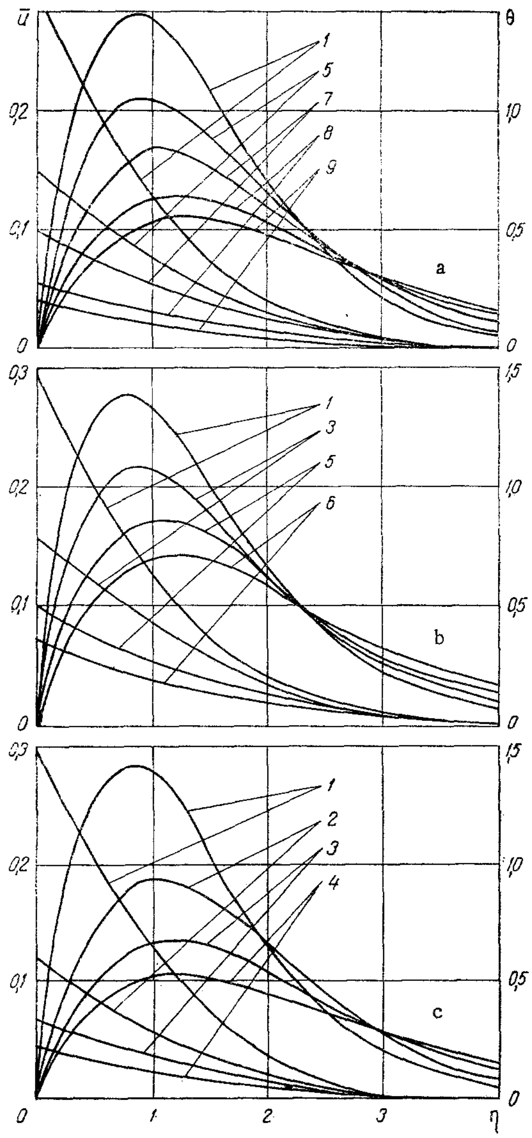

Fig. 1. Dimensionless velocity and temperature profiles in the boundary layer. a) R = 0; b) 5; c) 50; 1) $\xi = 0$; 2) 0.05; 3) 0.1; 4) 0.15; 5) 0.2; 6) 0.3; 7) 0.4; 8) 0.8; 9) 1.2.

From the equation of continuity we form the stream function and in problem (1)-(4) change over to the variables [3]

$$\psi(x,\ y) = 5\nu\left(\frac{\mathrm{Gr}_x^*}{5}\right)^{1/5} F(\xi,\ \eta),\quad \eta = \left(\frac{\mathrm{Gr}_x^*}{5}\right)^{1/5}\frac{y}{x},$$

$$T - T_\infty = \frac{q_w x}{\lambda}\left(\frac{\mathrm{Gr}_x^*}{5}\right)^{-1/5}\Theta(\xi,\ \eta),\quad \xi = \frac{\sigma\varepsilon T_\infty^3}{\lambda}\,x\left(\frac{\mathrm{Gr}_x^*}{5}\right)^{-1/5}, \tag{5}$$

which generalize the self-similar variables of the free-convection problem for a plane surface with constant heat flux [4].

Now problem (1)-(4) takes the form

$$\frac{\partial^3 F}{\partial\eta^3} + 4F\frac{\partial^2 F}{\partial\eta^2} - 3\left(\frac{\partial F}{\partial\eta}\right)^2 + \Theta = \xi\left(\frac{\partial E}{\partial\eta}\cdot\frac{\partial^2 F}{\partial\eta\partial\xi} - \frac{\partial F}{\partial\xi}\cdot\frac{\partial^2 F}{\partial\eta^3}\right). \tag{6}$$

$$\frac{1}{\mathrm{Pr}}\cdot\frac{\partial^2\Theta}{\partial\eta^2} + 4F\frac{\partial\Theta}{\partial\eta} - \Theta\frac{\partial F}{\partial\eta} = \xi\left(\frac{\partial F}{\partial\xi}\cdot\frac{\partial\Theta}{\partial\eta} - \frac{\partial F}{\partial\eta}\cdot\frac{\partial\Theta}{\partial\xi}\right), \tag{7}$$

$$F = \frac{\partial F}{\partial\eta} = 0,\quad \frac{\partial\Theta}{\partial\eta} = -1 + \xi\Theta(2 + R\xi\Theta)(2 + 2R\xi\Theta + R^2\xi^2\Theta^2)\ \text{for}\ \eta = 0, \tag{8}$$

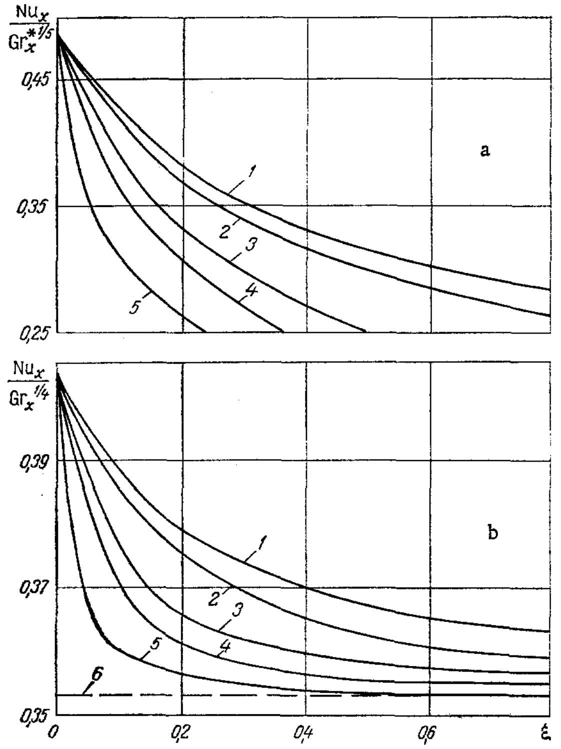

Fig. 2. Local heat-transfer criteria $Nu_x/Gr_x^{*1/5}$ (a) and $Nu_x/Gr_x^{1/4}$ versus longitudinal coordinate. 1) R = 0; 2) 1; 3) 5; 4) 10; 5) 50; 6) T_w = const.

$$\frac{\partial F}{\partial \eta} = 0, \quad \Theta = 0 \quad \text{for} \quad \eta \to \infty.$$

For $\xi = 0$ the derived equations go over to the system of ordinary differential equations for the self-similar nonradiative heat-transfer problem for a plate. The parameter $R = q_w/\sigma\varepsilon T_\infty^4$ characterizes the ratio between the total heat flux transported from the wall surface and the radiative component. The dimensionless longitudinal coordinate ξ establishes a connection between the radiative and convective components of the heat flux.

Near the leading edge the temperature differentials in the boundary layer are slight, and the free-convective component of the heat flux takes the dominant role in heat transfer from the wall. In the upper part of the plate the boundary layer grows thicker, and the heat flux due to convection gradually diminishes, while the radiative component increases. Inasmuch as the latter does not depend on the thickness of the boundary layer, but is determined by the surface temperature, it may be assumed that the surface temperature tends to a certain constant value T_W. The latter can be determined from the limiting value of the boundary condition $(\partial T/\partial y)_W = 0$ as $x \to \infty$; $T_W = T_\infty(1 + R)^{1/4}$ for $x \to \infty$.

Expanding the right-hand side into a series for small values of R, we obtain for the temperature differential in the boundary layer at large distances from the leading edge

$$T_w - T_\infty = \frac{q_w}{4\sigma\varepsilon T_\infty^3} \quad \text{as} \quad x \to \infty. \tag{9}$$

The most practical approach, therefore, is to seek an asymptotic solution for $x \to \infty$ in the variables of the free-convection problem near a wall with constant temperature [3]:

$$\Psi(x, y) = 4\nu\left(\frac{Gr_x}{4}\right)^{1/4}\varphi(\zeta, \eta_t), \quad \eta_t = \frac{y}{x}\left(\frac{Gr_x}{4}\right)^{1/4},$$
$$T - T_\infty = \frac{q_w}{4\sigma\varepsilon T_\infty^3}G(\zeta, \eta_t), \quad \zeta = \xi^{5/4}. \tag{10}$$

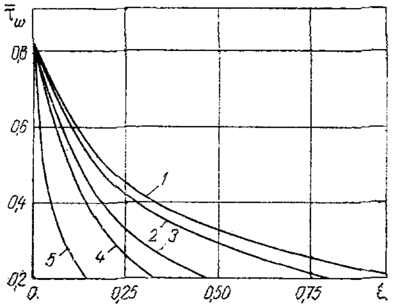
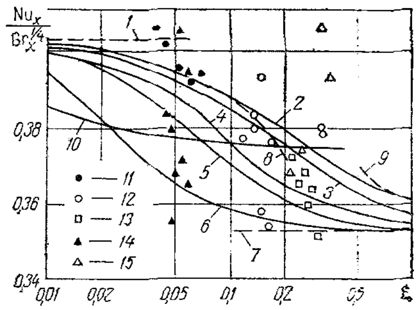

Fig. 3 Fig. 4

Fig. 3. Dimensionless frictional stress $\bar{\tau}_w$ versus longitudinal coordinate. 1) R = 0; 2) 1; 3) 5; 4) 10; 5) 50.

Fig. 4. Comparison of the results of calculations with experimental data on local heat transfer in the form $Nu_x Gr_x^{1/4}$. 1) q_w = const; 2) R = 0; 3) R = 1; 4) R = 5; 5) R = 10; 6) R = 50; 7) T_w = const; 8, 9) perturbation method [3]; 10) quasisteady asymptotic approximation method [7]. Experimental data: 11) ε = 0.96; 12) 0.52; 13) 0.20 [3]; 14) 0.197; 15) 0.98 [2].

Now Eqs. (1)-(4) assume the form

$$\frac{\partial^3\varphi}{\partial\eta_t^3} + 3\varphi\frac{\partial^2\varphi}{\partial\eta_t^2} - 2\left(\frac{\partial\varphi}{\partial\eta_t}\right)^2 + G = \zeta\left(\frac{\partial\varphi}{\partial\eta_t}\cdot\frac{\partial^2\varphi}{\partial\eta_t\partial\zeta} - \frac{\partial\varphi}{\partial\zeta}\cdot\frac{\partial^2\varphi}{\partial\eta_t^2}\right), \tag{11}$$

$$\frac{1}{\Pr}\cdot\frac{\partial^2 G}{\partial\eta_t^2} + 3\varphi\frac{\partial G}{\partial\eta_t} = \zeta\left(\frac{\partial\varphi}{\partial\eta_t}\cdot\frac{\partial G}{\partial\zeta} - \frac{\partial\varphi}{\partial\zeta}\cdot\frac{\partial G}{\partial\eta_t}\right), \tag{12}$$

$$\varphi = \frac{\partial\varphi}{\partial\eta_t} = 0,\quad \frac{\partial G}{\partial\eta_t} = -\frac{8}{5^{1/4}}\zeta\left\{\frac{1}{R}\left[\left(\frac{GR}{4}+1\right)^4 - 1\right] - 1\right\}$$

$$\text{for } \eta_t = 0, \tag{13}$$

$$\varphi = 0,\ G = 0 \quad \text{for } \eta_t \to \infty.$$

As $\zeta \to \infty$, Eqs. (11)-(13) go over to the self-similar problem for an isothermal plate with the following boundary condition for the dimensionless wall temperature:

$$G = \frac{4}{R}\left(\sqrt[4]{1+R} - 1\right) \quad \text{for } \eta_t = 0.$$

The radiative heat-transfer calculations are carried out mainly by approximative methods.

Cess [3] represents the solution of problem (6)-(8) in the form of two (zeroth and first) terms of a power series in ξ. The dependence on the parameter R shows up only in the second term of the series. Accordingly, Furman and Nenishev [5] represent the expansion as a double power series in the parameters ξ and R. However, the convergence of the resulting series is poor. The solution of the system (11)-(13) for large ξ can be represented as a power series in the quantity $\xi^{-5/4}$. Cess [3] has carried out numerical computations of the first term of the series on the assumption of a linearized radiation model:

$$\sigma\varepsilon\left(T_w^4 - T_\infty^4\right) = 4\sigma\varepsilon T_\infty^3\left(T_w - T_\infty\right).$$

In the presence of radiation the excess wall temperature can be approximated by a single-term power law with exponent n varying from 0 (constant temperature, $\xi \to \infty$) to 0.2 (constant heat flux, $\xi = 0$) [2, 5]. Approximate dependences of the parameter n on ε and R are obtained by processing of the experimental data [5] and numerical calculations of the complete system of equations (1)-(4) [2].

The calculations of [5] are carried out by a method close to the self-similar version and by an integral method with fourth-degree polynomials for the velocity and temperature distributions in the boundary layer. The problem has also been solved by the method of averaging of functional corrections [6].

The heat-transfer expressions are represented in implicit form and prove cumbersome for engineering calculations.

The method of quasisteady asymptotic approximation has been used [7] to calculate the dependence of the

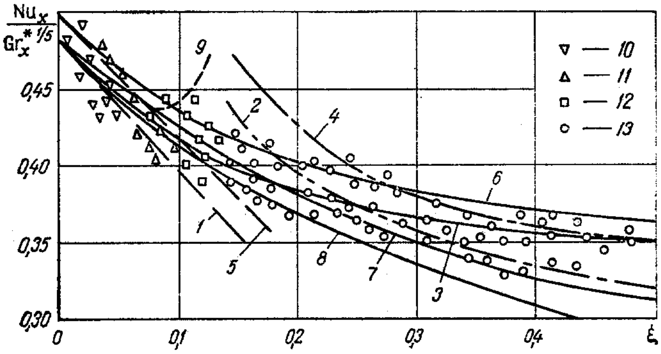

Fig. 5. Comparison of the results of calculations with experimental data on local heat transfer in the form $Nu_x/Gr_x^{*1/5}$. 1, 2) Perturbation method (first approximation [3]); 3) method close to the self-similar version [5]; 6, 5) integral method, limiting solutions [5]; 4) integral method; 7) R = 0; 8) R = 1; 9) perturbation method, second approximation [5]. Experimental data: 10) $\varepsilon = 0.131$; 11) 0.305; 12) 0.452; 13) 0.961 [5].

heat transfer on the variable $\xi^{5/4}(R/5\Pr)^{1/4}$. In the limits $\xi \to 0$ and $\xi \to \infty$ the numerical results are given with respective errors of 0.2 and 7%.

We have calculated the system of equations (6)-(8) numerically by a finite-difference technique. We use a six-point implicit difference scheme of second order with respect to ξ and η [8]. The nonlinear terms are linearized by simple iteration [9]. For example, the boundary condition for the dimensionless wall temperature is

$$\left(\frac{\partial\Theta}{\partial\eta}\right)^{i+1} = -1 + \xi\Theta^i(2 + R\xi\Theta^i)[2 + 2R\xi\Theta^i + R^2\xi^2(\Theta^i)^2].$$

The computations are carried out for Pr = 0.7 (air) and values of the radiation parameter R = 0, 1, 5, 10, and 50.

Distributions of the dimensionless velocities $\bar{u} = u/5\nu(Gr_x^*/5)^{2/5}x$ and temperatures Θ in the boundary layer for various values of the longitudinal coordinate ξ and radiation parameter R are given in Fig. 1. With increasing ξ the maximum velocity in the boundary layer decreases and shifts toward larger values of η. With increasing longitudinal coordinate the velocity and temperature profiles become increasingly flatter. The temperature and dynamic boundary layers evolve more rapidly the larger the value of R.

The local Nusselt number plotted according to the convective heat-flux component:

$$\frac{Nu_x}{(Gr_x^*)^{1/5}} = -\frac{1}{5^{1/5}\Theta_w}\left(\frac{\partial\Theta}{\partial\eta}\right)_w$$

decreases with ξ more rapidly for larger values of R (Fig. 2a). These curves are replotted in Fig. 2b in the variables of the fixed-temperature problem:

$$Nu_x/Gr_x^{1/4} = -\left(\frac{\partial\Theta}{\partial\eta}\right)_w/(5^{1/4}\Theta_w^{5/4}).$$

At $\xi = 0$ the curves merge into a single point, which corresponds to the heat transfer for a constant heat flux on the nonradiating surface. For large ξ the $Nu_x/Gr_x^{1/4}$ curves (Fig. 2b) tend to the limit corresponding to heat transfer for an isothermal plate. The asymptotic behavior of $Nu_x/Gr_x^{*1/5}$ as $\xi \to \infty$ is of another sort (Fig. 2a).

For large ξ the heat transfer from the plate can be calculated according to the dimensionless dependence for T_w = const. For example, the indicated heat-transfer dependence can be used with 2% error for $\xi > \exp(-0.49R^{0.51})$.

The ξ dependence of the dimensionless frictional stress at the wall $\bar{\tau}_w = \tau_w/(5\mu\nu/x^2)(Gr_x^*/5)^{3/5}$ is analogous to the variation of the local heat transfer (Fig. 3).

TABLE 1. Experimental Parameters

Physical quantity	Literature source [2]	[3]	[5]
$T_w - T_\infty$ (°K)	—	15—34	10—150
$q_w \left(\frac{W}{m^2}\right)$	269—529	$1{,}45 \cdot 10^5$	122—1854
Gr_L^*	—	—	$7{,}9 \cdot 10^4$—$5 \cdot 10^{10}$
Gr_L	—	$1{,}6 \cdot 10^7$—$1{,}3 \cdot 10^9$	—
ε	0,197;0,98	0,2—0,96	0,131—0,961
R	0,61—58	330—1580	0,12—19

The results of the calculations are compared with the experimental data in Figs. 4 and 5. The heat-transfer coefficient $Nu_x/Gr_x^{1/4}$ (Fig. 4) calculated by the perturbation method for Pr = 0.7 [3] agrees with the numerical solution for R = 0 within 1% error limits for $\xi < 0.15$ (curve 8) and $\xi > 0.5$ (curve 9). In the case of the quantity $Nu_x/Gr_x^{*1/5}$ agreement within the stated error limits obtains in a narrower range of values of ξ. The results obtained in the first perturbation approximation yield heat-transfer values that are too small for small ξ and too large for large ξ. In the second approximation [5] the heat-transfer values computed by the perturbation method agree well with the numerical calculations up to $\xi = 0.08$. (curve 9 in Fig. 5). The method close to the self-similar approach [5] gives values for the local heat-transfer coefficient that agree satisfactorily with the numerical solution for R = 0, 1 and $\xi < 0.2$, but gives excessive values for $\xi \to \infty$ (12% too high for $\xi = 0.6$) (curve 3 in Fig. 5). Approximately the same error occurs for the integral method [5] (curve 4) and the limiting solutions obtained by this method (curves 5 and 6). The values of $Nu_x Gr_x^{1/4}$ calculated by the quasi-steady asymptotic approximation method [7] exhibit poor agreement already for the limiting value $\xi \to \infty$ (curve 10 in Fig. 4).

The domain of variation of the parameters in the experimental investigations is given in Table 1. The shortage of initial experimental data [2, 3, 5] prevents us from collating all the experimental points on a single graph, and that is why the experimental heat-transfer data in the form of dependences of $Nu_x/Gr_x^{*1/5}$ and $Nu_x/Gr_x^{1/4}$ on ξ are presented in two figures. To compare the experimental with the analytical results for $Nu_x/Gr_x^{1/4}$ a high experimental accuracy is required, because the limits of variation of the dimensionless heat transfer over the entire range of ξ amount to 15%. In Fig. 4, however, the scatter of the experimental points is greater than this value. Although Cess [3] claims agreement within 8% between the theoretical and experimental results, the discrepancy is in fact much greater. Clearly, only the results for equal values of the parameter R can be legitimately compared. In [3], essentially, the theoretical curves for R = 0 are compared with experimental points for R = 330 to 1580.

The scatter of the experimental points is much smaller in Fig. 5, in which the calculations are compared with the experiments of [5] for $Nu_x/Gr_x^{*1/5}$.

It is noted that the experimental data agree with the numerical curves within 4 or 5% error limits for $0 < R < 1$.

Thus, the accuracy of the existing experiments is inadequate for a complete quantitative assessment of the applicability of the given simplified radiation model.

NOTATION

u, v, projections of velocity vector onto the X and Y axes; x, longitudinal coordinate; y, transverse coordinate; T, absolute temperature; q, heat flux; ν, kinematic viscosity coefficient; g, gravitational acceleration; β, coefficient of volume expansion; a, thermal diffusivity; λ, thermal conductivity; σ, Stefan–Boltzmann constant; ε, emissivity; α_x, local heat-transfer coefficient; τ_w, frictional stress at the wall; ψ, stream function; F, φ, Θ, G, dimensionless stream functions and temperatures; $\xi = (\sigma\varepsilon T_\infty^3 x/\lambda)(Gr_x^*/5)^{1/5}$, $\zeta = \xi^{5/4}$, dimensionless longitudinal coordinates; $\eta = (Gr_x^*/5)^{1/5}(y/x)$, $\eta_t = (Gr_x/4)^{1/4}(y/x)$, self-similar variables; $Gr_x^* = g\beta q_w x^4/\lambda\nu^2$, modified Grashof number; $Gr_x = g\beta q_w x^3/\nu^2 4\sigma\varepsilon T_\infty^3$, Grashof number; Pr, Prandtl number; Nu_x, Nusselt number; R, radiation parameter. Indices: x, local value; L, average value; ∞, far from surface; t, fixed temperature; j, iteration number; w, wall; 0, coordinate origin.

LITERATURE CITED

1. E. H. Cheng and M. N. Ozisik, Intern. J. Heat Mass Transfer, 25, No. 3 (1972).
2. W. G. England and A. F. Emery, Trans. ASME, Ser. C: J. Heat Transfer, 91, No. 1 (1969).
3. R. Cess, in: Advances in Heat Transfer, Vol. 1, Academic Press, New York (1963), pp. 1-50.
4. E. M. Sparrow and J. L. Gregg, Trans. ASME, Ser. C: J. Heat Transfer, 78, 435 (1956).
5. A. V. Furman and A. S. Nenishev, Izv. Akad. Nauk SSSR, Énerg. Transport, No. 3, 104 (1973).
6. V. V. Salomatov and E. M. Puzyrev, Inzh.-Fiz. Zh., 20, No. 6 (1968).
7. V. V. Salomatov and E. M. Puzyrev, in: Modern Problems of Thermal Gravitational Convection [in Russian], Nauka i Tekhnika, Minsk (1968).
8. S. K. Godunov and V. S. Ryaben'kii, Difference Schemes [in Russian], Nauka, Moscow (1973).
9. I. S. Berezin and I. P. Zhidkov, Computing Methods [in Russian], Vol. 2, Fizmatgiz, Moscow (1959).

NUMERICAL ANALYSIS OF SUPERSONIC FLOW OF AN IDEAL GAS IN THE WAKE OF AN AXISYMMETRICAL BODY

V. V. Bulanov

UDC 518:517.944/947

A numerical experiment is carried out on supersonic flow in the wake of an axisymmetrical body, and estimates are obtained for the "scheme" (artificial) viscosity introduced by a maximally stable difference scheme [1] into the investigated flow.

1. Statement of the Problem

Many papers have been published in the period from 1965 through 1975 on the numerical solution of problems involving the flow of a viscous liquid and a compressible gas in the wake of a body with separation points and reverse-circulation flow zones. In the majority of those papers the complete system of Navier — Stokes equations is approximated by a finite-difference scheme of first or second order, which is then solved by some suitable numerical or iterative technique.

However, solutions of the complete system of Navier — Stokes equations are obtained only for relatively small to moderate (values of a few hundred) Reynolds numbers (see, e.g., [3,4]). The numerical results obtained in these studies mainly corroborate the schematic representations of the flow pattern both in the separation zone and in the wake as a whole.

Very few results have been published on the numerical study of supersonic flows in the wakes of bodies at high and very high Reynolds numbers.

A modern approach that offers fuller understanding and investigation of the singular characteristics of flow at large Reynolds numbers is the application of shock-smearing (or shock-capturing) finite-difference schemes, which approximate the system of Euler equations rather than the complete system of Navier — Stokes equations (see, e.g., [5,6]).

The numerical solutions generated by such investigations may be viewed as numerical experiments, which correspond in their principal features to the true flow pattern for sufficiently large Reynolds numbers and yet are useful not only for the deeper insight that they offer into the singular flow characteristics at corners, in aft and wake zones, etc., but also for exhibiting the capabilities and singular characteristics of the difference scheme itself, for example the influence of the spatial mesh size of the computing grid, type of artificial viscosity, etc., on the accuracy of computation.

Translated from Inzhenerno-Fizicheskii Zhurnal, Vol. 32, No. 6, pp. 1080-1086, June, 1977. Original article submitted March 25, 1976.